Decomposition and Terapascal Phases of Water Ice

Chris J. Pickard* and Miguel Martinez-Canales
Department of Physics and Astronomy, University College London, Gower Street, London WC1E 6BT, United Kingdom

Richard J. Needs
Theory of Condensed Matter Group, Cavendish Laboratory, Cambridge CB3 0HE, United Kingdom
(Received 6 December 2012; revised manuscript received 23 March 2013; published 11 June 2013)

Computational searches for stable and metastable structures of water ice and other H:O compositions at TPa pressures have led us to predict that H_2O decomposes into H_2O_2 and a hydrogen-rich phase at pressures of a little over 5 TPa. The hydrogen-rich phase is stable over a wide range of hydrogen contents, and it might play a role in the erosion of the icy component of the cores of gas giants as H_2O comes into contact with hydrogen. Metallization of H_2O is predicted at a higher pressure of just over 6 TPa, and therefore H_2O does not have a thermodynamically stable low-temperature metallic form. We have also found a new and rich mineralogy of complicated water ice phases that are more stable in the pressure range 0.8–2 TPa than any predicted previously.

DOI: 10.1103/PhysRevLett.110.245701 PACS numbers: 64.70.K−, 61.50.Ks, 62.50.−p, 71.15.Mb

Water ice under high pressures is an important component of gas giant planets, and it has been speculated that it is present in the core of Jupiter at pressures as high as 6.4 TPa [1]. The pressures at the centers of massive exoplanets can reach 10 TPa or more [2], and establishing the properties of materials at TPa pressures is a very difficult task. Knowledge of the equation of state and whether the high-pressure phases are insulating or metallic is particularly important.

Hydrogen and oxygen are, respectively, the most abundant and the third most abundant elements in the solar system [3]. The spatial distributions of elements within planets are understood to some extent, but it is not in general known what chemical compounds are stable at TPa pressures. H_2O is a stable stoichiometry of the binary H:O system at low temperatures and pressures, and the reaction

$$H_2O \rightarrow H_yO_z + H_{2-y}O_{1-z}$$

is endothermic for all y and z, $0 < y < 2$, $0 < z < 1$.

TPa pressures are becoming more accessible experimentally, but it is not currently possible to determine the stable stoichiometries of materials at TPa pressures experimentally, or the crystalline structures of any compounds formed. We can, however, make progress using theoretical approaches. The capability to search for thermodynamically stable crystal structures using density functional theory (DFT) methods has developed rapidly in recent years. Here we report searches for stable structures of various H:O stoichiometries using DFT methods, which have allowed us to investigate the stability of H_2O and of other stoichiometries at TPa pressures.

Static-compression diamond-anvil-cell experiments have given us a great deal of information about water ice up to pressures of 0.21 TPa [4–6], but this is far below the highest pressures to which water is subjected within planets. Shock wave experiments can reach much higher pressures, and sample precompression [7,8] and ramped compression [9,10] techniques can reduce the resulting temperatures to those more appropriate for planetary science.

The low-pressure and low-temperature phases of ice consist of packing of hydrogen-bonded water molecules [11]. Compression of the high-pressure molecular ice VIII phase leads to a transition at about 0.1 TPa to the ice X structure, in which the H atoms move to the midpoints between neighboring O atoms and the molecules lose their separate identities [12]. Ice X is the highest-pressure phase that has been observed experimentally, but DFT studies have predicted further phase transitions at higher pressures [13–17]. The structural chemistry of some of these phases is discussed in Ref. [18].

We have performed DFT calculations [19] of structures with various H:O stoichiometries using the CASTEP [20] plane-wave code, the Perdew-Burke-Ernzerhof (PBE) [21] generalized gradient approximation density functional, and ultrasoft pseudopotentials [22]. We searched for low enthalpy structures using the *ab initio* random structure searching (AIRSS) method [23,24]. This method has been applied to many systems including H_2O at low pressures [25], and hydrogen [26–28] and oxygen [29] at high pressures. AIRSS involves choosing starting structures and relaxing each of them to a minimum in the enthalpy. We have made extensive use of symmetry constraints in our searches. Starting structures were generated conforming to a particular space group symmetry, although they were otherwise random, and they were relaxed while maintaining the symmetry constraint. We performed searches for H_2O structures with up to 16 formula units (f.u.), and searches for other stoichiometries were performed with up to 98 atoms [19].

The stability ranges of the most energetically favorable phases of H_2O are given in Table I, including those found in earlier DFT studies [13–17]. The AIRSS calculations produced three water-ice structures of symmetries $P3_121$ (or its chiral enantiomorph $P3_212$), $Pcca$, and $C2$, with lower static-lattice enthalpies within the pressure range 0.78–2.36 TPa than those known previously; see Table I and Ref. [19]. We also found the $Pmc2_1$ structure reported by McMahon [15] and the $I\bar{4}2d$ phase of Ref. [17], but they are metastable on our phase diagram. At higher pressures we found the $P2_1$ [15–17], $P2_1/c$ [16], and $C2/m$ [15] structures of earlier studies. Theoretical predictions of still higher pressure phases have been reported but, as we show below, they are not stable [30]. We also performed calculations using the local density approximation (LDA) [31] for the $Pbca \leftrightarrow P3_121$ and $P2_1/c \leftrightarrow C2/m$ transitions, which gave transition pressures similar to those using the PBE functional [19]. The LDA and PBE functionals have been tested successfully in many high-pressure studies. The pseudovalence electronic charge densities of materials become more uniform at very high pressures, and the LDA and PBE functionals are particularly appropriate under such conditions because they obey the uniform limit and give an excellent description of the linear response of the electron gas to an applied potential [21]. Additional discussion of these issues for carbon at TPa pressures is presented in the Supplemental Material for Ref. [32].

It is important to include the quantum nuclear zero-point (ZP) motion when considering the energetics of systems containing light atoms. We therefore calculated the vibrational modes of the most stable phases within the quasiharmonic approximation and evaluated the corresponding contributions to the free energies and pressures. Technical details of the phonon calculations are given in the Supplemental Material [19]. The enthalpy-pressure relations of the relevant phases, including ZP motion, are shown in Fig. 1. (The enthalpy reduction arising from the $Pbcm$ distortion is too small to be visible on the scale of Fig. 1.) When ZP motion effects are included, the $C2$ and $P2_1$ phases no longer have regions of thermodynamic stability, and our $P3_121$ and $Pcca$ phases become stable in the ranges 0.77–1.44 TPa and 1.44–1.93 TPa, respectively. Figure 2 shows the computed phase diagram including vibrational motion up to 2000 K. Note that our predicted pressure for the onset of stability of $P3_121$ H_2O of 0.77 TPa is not much higher than that of 0.7 TPa achieved in recent shock compression of water [33], and that static compression of rhenium up to 0.64 TPa was recently achieved in a secondary anvil diamond cell [34], so that the pressures considered here are likely to become accessible in the future.

TABLE I. Space group symmetries, calculated stability ranges, and numbers of f.u. per primitive unit cell for phases of H_2O. Nuclear vibrational motion is not included in this data. The right-hand column gives the source of the structure.

Space group	Stability range (TPa)	No. f.u.	Source
Ice X	–0.30	2	Ref. [12]
$Pbcm$	0.30–0.71	4	Ref. [13]
$Pbca$	0.71–0.78	8	Ref. [14]
$P3_121$	0.78–2.01	12	This work
$Pcca$	2.01–2.24	12	This work
$C2$	2.24–2.36	12	This work
$P2_1$	2.36–2.75	4	Refs. [15–17]
$P2_1/c$	2.75–6.06	8	Ref. [16]
$C2/m$	6.06–	2	Ref. [15]

The $Pbcm$, $Pbca$, $P2_1$, $P2_1/c$, $C2/m$, and $I\bar{4}2d$ structures have been described in previous work [13–17]. The O atoms of the $P3_121$ structure form hexagonal-close-packed layers, which are stacked not in the middle of the triangles of the adjacent layers but midway along an edge, with a three-layer repeat; see Fig. 3. The density increases by about 2% at the transition from $Pbca$ to $P3_121$, which is reflected in the substantial reduction in the gradient of the enthalpy-pressure curve at the transition apparent in Fig. 1. The O lattice of the layered $Pcca$ structure exhibits a quartzlike "bow tie" motif [19], and it is not particularly similar to any of the standard close-packed structures. The primitive cells of the $P3_121$ and $Pcca$ structures are large, containing 12 f.u., and they appear to be of previously unknown structure types. The $C2$ structure also exhibits the bow tie motif. Details of the $P3_121$, $Pcca$, and $C2$ structures are reported in the Supplemental Material [19].

H_2O and H_2 readily form hydrogen clathrate compounds at low pressures [35]. Much denser structures are favored at high pressures, which can lead to changes in bonding and/or decomposition into compounds of other stoichiometries,

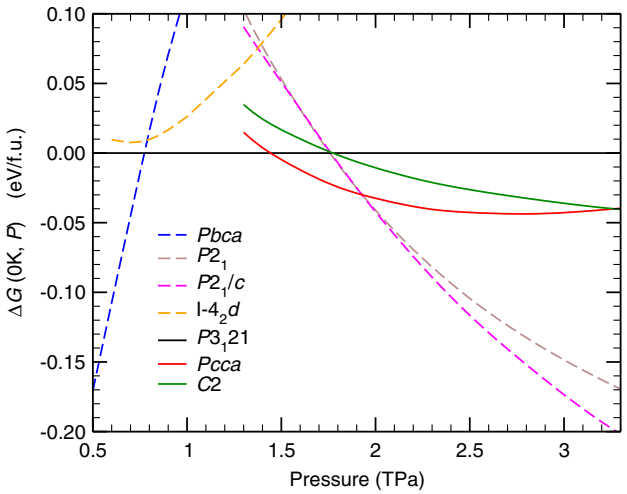

FIG. 1 (color online). Variation of the enthalpies with pressure of high-pressure water-ice structures. Previously known structures are indicated by dashed lines, and phases that we have predicted are shown as solid lines. ZP motion is included at the quasiharmonic level.

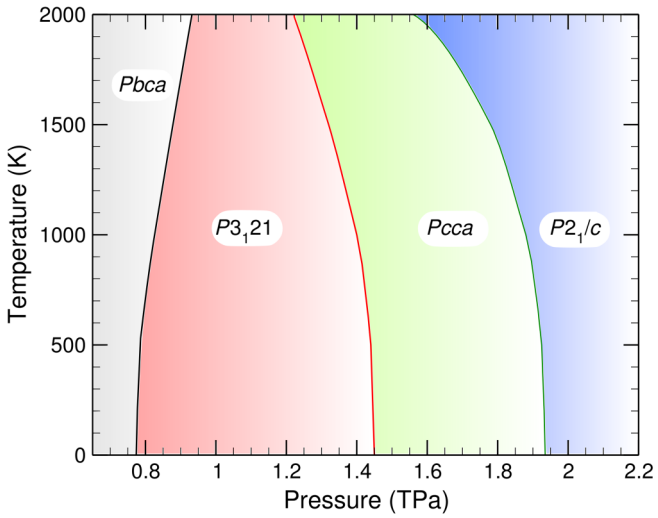

FIG. 2 (color online). Phase diagram of water ice including vibrational motion.

and a recent study has shown that H:O compounds other than H_2O may be stable at TPa pressures [30]. For example, we have identified a high-symmetry, well-packed, very stable and insulating structure of hydrogen peroxide (H_2O_2) of space group $Pa\bar{3}$; see Fig. 3, which contains O-O bonds and threefold coordinated H atoms. We have found that this phase plays an important role in determining the stability of H_2O at high pressures.

We have searched over various H:O stoichiometries to investigate the stability of H_2O to decomposition at TPa pressures. We found an instability of H_2O at pressures a little above 5 TPa to a decomposition of the form

$$H_2O \rightarrow \frac{\delta}{1+\delta}\frac{1}{2}H_2O_2 + \frac{1}{1+\delta}H_{2+\delta}O, \qquad (1)$$

with $\delta \geq 1/8$. The right-hand side of this reaction equation is simply H_2O when $\delta = 0$, but for $\delta > 0$ it corresponds to the formation of H_2O_2 and a hydrogen-rich $H_{2+\delta}O$ compound.

This instability is illustrated in more detail in the convex hull diagram of Fig. 4(a). At high pressures the $Pa\bar{3}$ H_2O_2 structure is on the convex hull at $x = 0$. At 4 TPa, which is below the instability to decomposition, the $P2_1/c$ phase of water ice is on the convex hull and is stable. At 6 TPa the $P2_1/c$ and $C2/m$ phases are almost degenerate and the convex hull passes below them, and all H_2O structures are unstable to decomposition. This decomposition is shown in Eq. (1), and it leads to the formation of $H_2O_2 + H_{2+1/8}O$, so that $\delta = 1/8$. Note, however, that the enthalpies of hydrogen-rich structures from $\delta = 1/8$ up to about $\delta = 5/12$ are on the convex hull and they are therefore also stable at 6 TPa. Some of the most stable structures that we have found with fractional values of δ have large unit cells containing up to 98 atoms. It is likely that a quasicontinuum of structures with different values of δ are stable

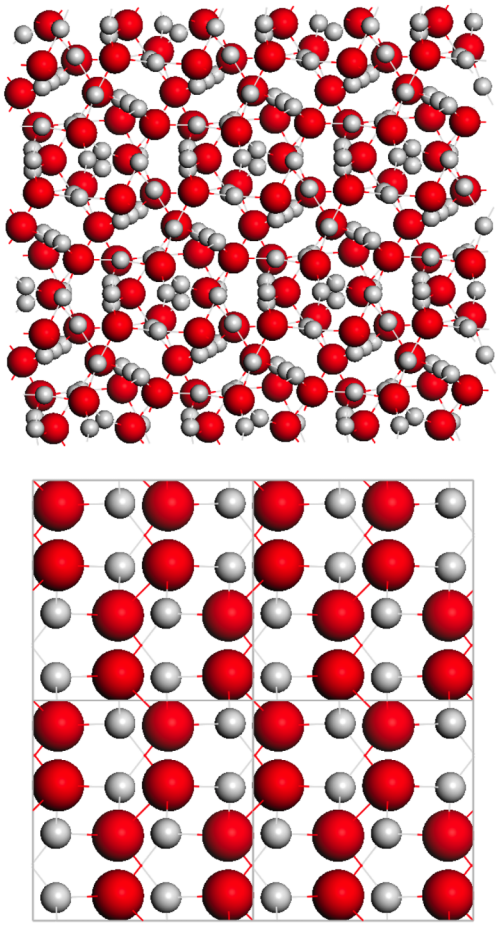

FIG. 3 (color online). Top: $P3_121$ structure of water ice at 1 TPa. Bottom: $Pa\bar{3}$ structure of H_2O_2 at 6 TPa. The O atoms are shown in red and the H atoms in gray.

at 6 TPa. We have also calculated the enthalpies of the structures at 5 TPa, and find that this pressure is close to, but just below, the lowest pressure at which H_2O decomposes. We therefore conclude that, at low temperatures, H_2O becomes unstable to decomposition at pressures of a little above 5 TPa.

From $\delta = 0$ up to somewhere between $\delta = 1/4$ and $1/2$ the hydrogen-rich $H_{2+\delta}O$ structures resemble the $C2/m$ phase, but with layers of H atoms inserted; see Fig. 4(b). We also found hydrogen deficient $C2/m$ variants, but they are not stable under the conditions studied here. The appearance of structures with $\delta \neq 0$ can be understood as a topotactic transition [36] to structures in which the O lattice is maintained, while the $C2/m$-like structures differ in the amount of hydrogen incorporated. These phases might be described as interstitial solid solutions.

The $H_{2+\delta}O$ phases are weakly metallic [19]. The relative enthalpies of the $H_{2+\delta}O$ phases correlate with the density of electronic states at the Fermi energy [eDOS(E_F)]. The eDOS(E_F) takes its minimum value at $\delta = 1/4$, which corresponds to the minimum in the convex hull of Fig. 4; see also Ref. [19]. This suggests that the

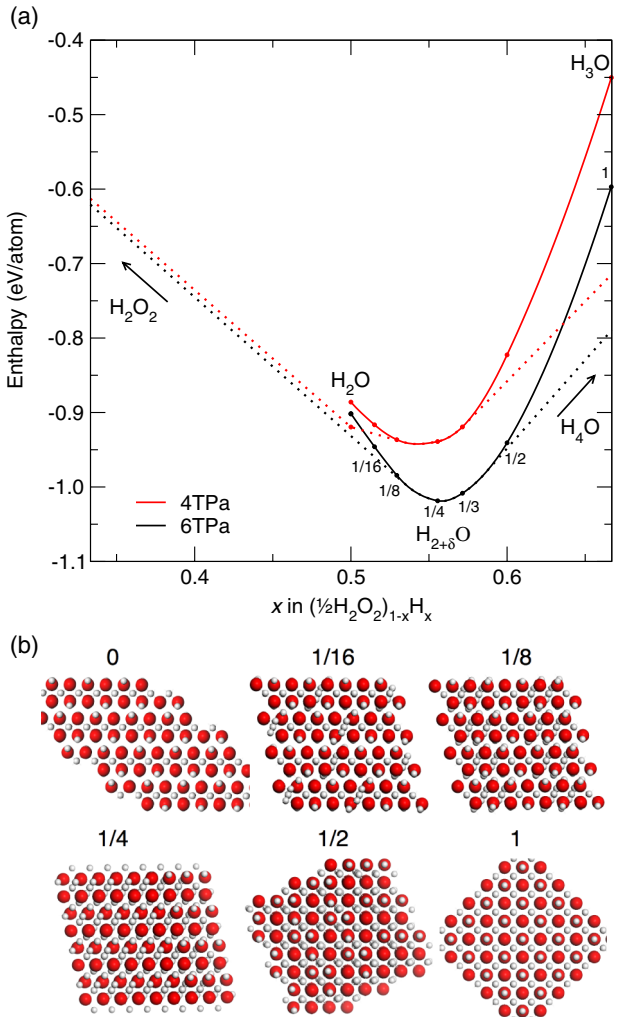

FIG. 4 (color online). (a) Convex hull diagram and enthalpies of $(1/2H_2O_2)_{1-x}H_x$ structures. The upper (red) and lower (black) broken lines show the convex hulls at 4 and 6 TPa, respectively. The upper (red) and lower (black) solid lines show the enthalpies of selected structures at 4 and 6 TPa, respectively. At 4 TPa the $P2_1/c$ phase [lower dot at $x = 0.5$ (red)] is more stable than $C2/m$ [upper dot at $x = 0.5$ (red)]. At 6 TPa the $P2_1/c$ and $C2/m$ phases are almost degenerate [middle dot at $x = 0.5$ (black)]. Six values of δ are labelled on the enthalpy curves, and the enthalpies of the corresponding structures for $\delta \simeq 1/8$ to $\delta \simeq 5/12$ lie on the convex hull at 4 and 6 TPa. (b) Six $H_{2+\delta}O$ structures at 6 TPa with values of δ from 0 to 1/2, with O atoms shown as large balls (red) and H atoms as small balls (gray). These structures have very similar arrangements of O atoms for $\delta = 0$ to 1/4, but between $\delta = 1/4$ and 1/2 the O packing changes to bcc.

relative stability of the $H_{2+\delta}O$ phases is connected with the Fermi surface or Bragg plane mechanism [37], in which the energy is reduced by the formation of a pseudogap in the eDOS around E_F arising from a symmetry breaking mechanism, which in this case involves the insertion of H atoms. It is possible that the true ground states of the $H_{2+\delta}O$ phases could be incommensurate charge-density-wave metals with wavelengths related to the Fermi surface.

If H_2O occurs under conditions of excess hydrogen, for example, at the core-mantle boundary in a gas giant planet, the metallic hydrogen-rich $C2/m$-like and bcc-like phases that we have found could act as "hydrogen sponges," soaking up hydrogen from the mantle. We suggest that such a mechanism might play a role in erosion of the ice component in the core of gas giants as H_2O comes into contact with H_2. Entropic effects also favor dissolution of H:O compounds in hydrogen at high temperatures [38].

In summary, we have found a new and rich mineralogy of complicated water-ice phases of previously unknown structure types, which lead to a revision of the predicted phase diagram of H_2O within the pressure range of about 0.8–2 TPa and above 5 TPa. We predict that H_2O decomposes into H_2O_2 and hydrogen-rich phases based on the layered $C2/m$ structure of H_2O and on phases with a bcc O lattice at pressures a little above 5 TPa. This suggests that H_2O is not a stable compound at the highest pressures at which it has been suggested to occur within Jupiter. We suggest that the $C2/m$ structure might play a role in the erosion of icy cores of gas giant planets. The insulator-metal transition is predicted to occur at the transition from $P2_1/c$ to $C2/m$, but H_2O is unstable to decomposition at this pressure, and therefore it does not have a thermodynamically stable low-temperature metallic form. Our study supports previous suggestions that icy planetary cores could be strongly eroded by contact with a hydrogen-rich mantle [38–40].

We acknowledge financial support from the Engineering and Physical Sciences Research Council (EPSRC) of the United Kingdom, and the use of the UCL Legion High Performance Computing Facility, and associated support services. We thank Sian Dutton for helpful discussions.

*c.pickard@ucl.ac.uk

[1] B. Militzer, W. B. Hubbard, J. Vorberger, I. Tamblyn, and S. A. Bonev, Astrophys. J. Lett. **688**, L45 (2008).
[2] The Extrasolar Planets Encyclopaedia, http://exoplanet.eu/.
[3] D. Arnett, *Supernovae and Nucleosynthesis* (Princeton University, Princeton, NJ, 1996).
[4] R. J. Hemley, A. P. Jephcoat, H.-K. Mao, C. S. Zha, L. W. Finger, and D. E. Cox, Nature (London) **330**, 737 (1987).
[5] A. F. Goncharov, V. V. Struzhkin, M. S. Somayazulu, R. J. Hemley, and H.-K. Mao, Science **273**, 218 (1996).
[6] P. Loubeyre, R. LeToullec, E. Wolanin, M. Hanfland, and D. Hausermann, Nature (London) **397**, 503 (1999).
[7] K. K. M. Lee, L. R. Benedetti, R. Jeanloz, P. M. Celliers, J. H. Eggert, D. G. Hicks, S. J. Moon, A. Mackinnon, L. B. Da Silva, D. K. Bradley, W. Unites, G. W. Collins, E. Henry, M. Koenig, A. Benuzzi-Mounaix, J. Pasley, and D. Neely, J. Chem. Phys. **125**, 014701 (2006).

[8] R. Jeanloz, P. M. Celliers, G. W. Collins, J. H. Eggert, K. K. M. Lee, R. S. McWilliams, S. Brygoo, and P. Loubeyre, Proc. Natl. Acad. Sci. U.S.A. **104**, 9172 (2007).
[9] J.-P. Davis, C. Deeney, M. D. Knudson, R. W. Lemke, T. D. Pointon, and D. E. Bliss, Phys. Plasmas **12**, 056310 (2005).
[10] J. Hawreliak, J. Colvin, J. Eggert, D. H. Kalantar, H. E. Lorenzana, S. Pollaine, K. Rosolankova, B. A. Remington, J. Stölken, and J. S. Wark, Astrophys. Space Sci. **307**, 285 (2007).
[11] C. G. Salzmann, P. G. Radaelli, E. Mayer, and J. L. Finney, Phys. Rev. Lett. **103**, 105701 (2009).
[12] A. Polian and M. Grimsditch, Phys. Rev. Lett. **52**, 1312 (1984).
[13] M. Benoit, M. Bernasconi, P. Focher, and M. Parrinello, Phys. Rev. Lett. **76**, 2934 (1996).
[14] B. Militzer and H. F. Wilson, Phys. Rev. Lett. **105**, 195701 (2010).
[15] J. M. McMahon, Phys. Rev. B **84**, 220104 (2011).
[16] M. Ji, K. Umemoto, C.-Z. Wang, K.-M. Ho, and R. M. Wentzcovitch, Phys. Rev. B **84**, 220105 (2011).
[17] Y. Wang, H. Liu, J. Lv, L. Zhu, H. Wang, and Y. Ma, Nat. Commun. **2**, 563 (2011).
[18] A. Hermann, N. W. Ashcroft, and R. Hoffmann, Proc. Natl. Acad. Sci. U.S.A. **109**, 745 (2011).
[19] See Supplemental Material at http://link.aps.org/supplemental/10.1103/PhysRevLett.110.245701 for more details of the calculations, structures, electronic structures, and phonon dispersion relations.
[20] S. J. Clark, M. D. Segall, C. J. Pickard, P. J. Hasnip, M. I. J. Probert, K. Refson, and M. C. Payne, Z. Kristallogr. **220**, 567 (2005).
[21] J. P. Perdew, K. Burke, and M. Ernzerhof, Phys. Rev. Lett. **77**, 3865 (1996).
[22] D. Vanderbilt, Phys. Rev. B **41**, 7892 (1990).
[23] C. J. Pickard and R. J. Needs, Phys. Rev. Lett. **97**, 045504 (2006).
[24] C. J. Pickard and R. J. Needs, J. Phys. Condens. Matter **23**, 053201 (2011).
[25] C. J. Pickard and R. J. Needs, J. Chem. Phys. **127**, 244503 (2007).
[26] C. J. Pickard and R. J. Needs, Nat. Phys. **3**, 473 (2007).
[27] J. M. McMahon and D. M. Ceperley, Phys. Rev. Lett. **106**, 165302 (2011).
[28] C. J. Pickard, M. Martinez-Canales, and R. J. Needs, Phys. Rev. B **85**, 214114 (2012); **86**, 059902(E) (2012).
[29] J. Sun, M. Martinez-Canales, D. D. Klug, C. J. Pickard, and R. J. Needs, Phys. Rev. Lett. **108**, 045503 (2012).
[30] S. Zhang, H. F. Wilson, K. P. Driver, and B. Militzer, Phys. Rev. B **87**, 024112 (2013).
[31] J. P. Perdew and A. Zunger, Phys. Rev. B **23**, 5048 (1981).
[32] M. Martinez-Canales, C. J. Pickard, and R. J. Needs, Phys. Rev. Lett. **108**, 045704 (2012).
[33] M. D. Knudson, M. P. Desjarlais, R. W. Lemke, T. R. Mattsson, M. French, N. Nettelmann, and R. Redmer, Phys. Rev. Lett. **108**, 091102 (2012).
[34] L. Dubrovinsky, N. Dubrovinskaia, V. B. Prakapenka, and A. M. Abakumov, Nat. Commun. **3**, 1163 (2012).
[35] W. L. Mao, H.-k. Mao, A. F. Goncharov, V. V. Struzhkin, Q. Guo, J. Hu, J. Shu, R. J. Hemley, M. Somayazulu, and Y. Zhao, Science **297**, 2247 (2002).
[36] R. D. Shannon and R. C. Rossi, Nature (London) **202**, 1000 (1964).
[37] H. Jones, Proc. R. Soc. A **147**, 396 (1934).
[38] H. F. Wilson and B. Militzer, Astrophys. J. **745**, 54 (2012).
[39] D. J. Stevenson, Planet. Space Sci. **30**, 755 (1982).
[40] T. Guillot, Science **286**, 72 (1999).